The American Journal of Pathology, Vol. 193, No. 3, March 2023

ELSEVIER

The American Journal of
PATHOLOGY
ajp.amjpathol.org

CARDIOVASCULAR, PULMONARY, AND RENAL PATHOLOGY

Deficiency of the Planar Cell Polarity Protein Intu Delays Kidney Repair and Suppresses Renal Fibrosis after Acute Kidney Injury

Shixuan Wang,* Aimin Liu,† Yunchao Su,‡§ and Zheng Dong*§

From the Departments of Cellular Biology and Anatomy and Pharmacology and Toxicology,‡ Medical College of Georgia at Augusta University, Augusta, Georgia; the Department of Biology,† Eberly College of Sciences, Huck Institute of the Life Sciences, The Pennsylvania State University, University Park, Pennsylvania; and Research Department,§ Charlie Norwood VA Medical Center, Augusta, Georgia*

Accepted for publication December 6, 2022.

Address correspondence to Zheng Dong, Ph.D., or Shixuan Wang, M.D., Ph.D., Department of Cellular Biology and Anatomy, Medical College of Georgia at Augusta University and Charlie Norwood VA Medical Center, Augusta, GA 30912.
E-mail: zdong@augusta.edu or shwang@augusta.edu.

Planar cell polarity (PCP), a process of coordinated alignment of cell polarity across the tissue plane, may contribute to the repair of renal tubules after kidney injury. Intu is a key effector protein of PCP. Herein, conditional knockout (KO) mouse models that ablate *Intu* specifically from kidney tubules (*Intu* KO) were established. *Intu* KO mice and wild-type littermates were subjected to unilateral renal ischemia/reperfusion injury (IRI) or unilateral ureteral obstruction. Kidney repair was evaluated by histologic, biochemical, and immunohistochemical analyses. *In vitro*, scratch wound healing was examined in *Intu*-knockdown and control renal tubular cells. Ablation of *Intu* in renal tubules delayed kidney repair and ameliorated renal fibrosis after renal IRI. *Intu* KO mice had less renal fibrosis during unilateral ureteral obstruction. Mechanistically, *Intu* KO kidneys had less senescence but higher levels of cell proliferation and apoptosis during kidney repair after renal IRI. *In vitro*, *Intu* knockdown suppressed scratch wound healing in renal tubular cells, accompanied by the abnormality of centrosome orientation. Together, the results provide the first evidence for the involvement of PCP in tubular repair after kidney injury, shedding light on new strategies for improving kidney repair and recovery. *(Am J Pathol 2023, 193: 275–285; https://doi.org/10.1016/j.ajpath.2022.12.006)*

Acute kidney injury (AKI) is a clinical syndrome characterized by the abrupt decline of renal function, resulting from sepsis, renal ischemia/reperfusion, or exposure to nephrotoxins.[1,2] In spite of current technology and hospital care, AKI is accompanied by high rates of mortality and morbidity. Patients who survive the acute phase of AKI bear a long-term recovery stage, and some may progress to chronic kidney disease.[1–3] Tubular damage is a key pathologic feature of AKI.[4] While complete repair of damaged tubules restores full functionality, partial or maladaptive tubule repair leads to the development of chronic kidney problems, such as chronic inflammation and renal fibrosis. Therefore, kidney repair after AKI is centered on the repair and reconstruction of renal tubules.[2,4–8]

Planar cell polarity (PCP) refers to the coordinated alignment of cell polarity across the plane of the tissue. Especially, PCP is a determinant of the orientation of cell division, and as a result, plays an essential role in embryonic and organ development.[9–16] Following kidney injury, renal tubular repair involves dedifferentiation, migration, proliferation, and redifferentiation of surviving tubular cells to reconstruct the tubule. In this process, cell division needs to be oriented longitudinally; otherwise, tubular cell proliferation may lead to the expansion of the lumen, resulting in cyst formation.[17] Therefore, PCP is hypothesized to be a potentially important cellular event in tubular repair.

PCP is governed by a complex molecular machinery consisting of two-module network (core and Fat protein

Supported by NIH grants DK058831 and DK087843; and the US Department of Veterans Affairs grant BX000319. Z.D. is a recipient of senior Career Research Scientist award of the US Department of Veteran Affairs.

Disclosures: None declared.

https://doi.org/10.1016/j.ajpath.2022.12.006

systems) and effector proteins.[9–15] Intu is a key PCP effector protein that accumulates at the base of cilia and basal body in *Drosophila*.[18,19] Disruption of *Intu* in *Xenopus* and mouse leads to defects in cilia and neural tube closure.[20,21] Recent work[18] further discovered several *INTU* mutations in patients with ciliopathy, a set of diseases associated with dysfunctional cilia. Intu protects kidney from ischemic AKI by interacting with, and inducing the degradation of, Stat1.[22] However, the role of Intu and associated PCP in kidney repair is unknown.

This study was designed to delineate the involvement of PCP in kidney repair after injury. Especially, conditional knockout (KO) mouse models were established where the PCP effector *Intu* was ablated specifically from renal tubules. KO of *Intu* delayed kidney recovery and ameliorated renal fibrosis after ischemia/reperfusion injury (IRI). These mice developed less renal fibrosis during unilateral ureteral obstruction (UUO). Mechanistically, *Intu* KO suppressed senescence but increased cell proliferation and apoptosis in kidney tissues after renal IRI. In cultured renal tubular cells, knockdown of *Intu* inhibited wound healing in a scratch model. These results support a role for PCP in tubular repair after injury in kidney diseases.

Materials and Methods

Antibodies and Reagents

Primary antibodies were from following sources: Abcam (Waltham, MA): fibronectin (number ab2413), α-smooth muscle actin (number ab5694), Ser-139 phosphorylated H2A histone family member X (γ-H2AX; number ab26350), cyclophilin B (number ab16045), and p16 (number ab54210); Cell Signaling (Danvers, MA): cleaved caspase-3 (number 9661), vimentin (number 3932), and Ki-67 (number 9129); Sigma (St. Louis, MO): acetylated tubulin (number 7451), γ-tubulin (number T5326), and β-actin (number A2228); Novus Biologicals (Centennial, CO): collagen 1a1 (number NBP1-30054); Santa Cruz Biotech (Dallas, TX): α-tubulin (number sc-23948); and R&D Systems (Minneapolis, MN): kidney injury molecule 1 (Kim1; number AF1817). The primary antibody for Intu was generated as indicated in a previous study.[22] Secondary antibodies for immunoblot analysis were from Jackson ImmunoResearch (West Grove, PA); and for immunofluorescence staining, from Chemicon (Temecula, CA). Other reagents were from Sigma, unless specifically indicated.

Animal Models

Mice were housed in the animal facility of the Charlie Norwood VA Medical Center (Augusta, GA). Two animal models (IRI and UUO) were used. All animal experiments were performed according to a protocol approved by the Institutional Animal Care and Use Committee of the Charlie Norwood VA Medical Center.

Inducible *Intu* KO Mouse Model

For generation of the inducible *Intu* KO mice, floxed *Intu* ($Intu^{f/f}$) mice were crossed with mice harboring kidney tubule–specific and inducible Cre ($Pax8^{+/-}$,$LC1^{+/-}$)[23] to produce heterozygous mice ($Intu^{f/-}$,$Pax8^{+/-}$,$LC1^{+/-}$). Heterozygous mice were backcrossed with $Intu^{f/f}$ mice to generate wild-type ($Intu^{f/f}$,$Pax8^{+/-}$,$LC1^{-/-}$; $Intu^{f/f}$,$Pax8^{-/-}$,$LC1^{+/-}$) and KO ($Intu^{f/f}$,$Pax8^{+/-}$,$LC1^{+/-}$) mice. Genomic DNA was extracted from mouse tail/ear biopsy for PCR-based genotyping. The *Intu*-floxed allele product was detected at approximately 420 bp by PCR using three primers (forward: 5′-GATTAGGGTCTCGCCCTAGC-3′, reverse: 5′-ACAACCACAAGACTGCGTCA-3′, and reverse: 5′-ATGCACAAGTGTGTGGGTGT-3′). *Pax8* gene product was detected at approximately 600 bp by PCR using one pair of primers (forward: 5′-CCATGTCTAGACTGGACAAGA-3′ and reverse: 5′-CTCCAGGCCACATATGATTAG-3′). *LC1* gene product was detected at approximately 420 bp by PCR using one pair of primers (forward: 5′-TCGCTGCATTACCGGTCGATGC-3′ and reverse: 5′-CCATGAGTGAACGAACCTGGTCG-3′). Wild-type and KO male littermates (aged 2 to 3 months) were used for experiments.

Kidney Repair after Ischemic Injury

Renal ischemia was induced as previously described.[22] Right kidney underwent ischemia insult, and the left kidney was kept intact.[8,24] Briefly, mice were anesthetized with pentobarbital (60 mg/kg) and kept on a homoeothermic station to maintain body temperature at approximately 36.5°C. Buprenorphine (0.05 mg/kg) was administered as an analgesic for pain relief. Right kidneys were surgically exposed for renal pedicle clamping with arterial clips to induce renal ischemia. After 33 minutes of clamping, the arterial clips were released for reperfusion. Sham control mice were subjected to identical procedure but without renal pedicle clamping. At day 13 after surgery, left kidneys were removed. Mice were sacrificed at day 14 for the collection of right kidneys and blood.

Unilateral Ureteral Obstruction

Proximal tubule–specific *Intu* KO mice were generated by crossing *Intu* floxed mice[21,22] with PEPCK-Cre mice,[25] as described in our previous study.[22] Wild-type and KO male mice (aged 2 to 3 months) were used for this experiment. For UUO, the left ureter was exposed and ligated with 5-0 silk suture at two points of the ureter.

Sirius Red/Fast Green Collagen Staining

Kidney fibrosis was evaluated with Sirius red/fast green collagen staining kit (Chondrex, Woodinville, WA). Briefly, paraffin-embedded tissue sections were deparaffinized by

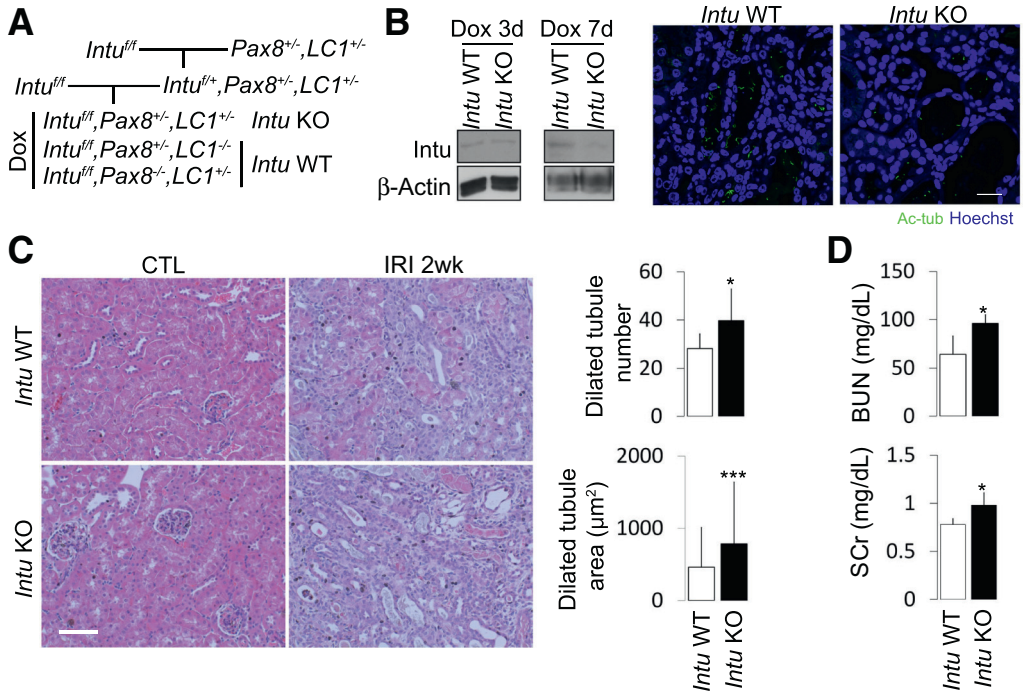

Figure 1 Knockout (KO) of tubular *Intu* after ischemia/reperfusion injury (IRI) suppresses kidney repair. **A:** Breeding scheme for establishing the inducible *Intu* knockout mouse model. Mice with floxed *Intu* ($Intu^{f/f}$) were mated with $Pax8^{+/-}$,$LC1^{+/-}$ transgenic mice for generating kidney tubule–specific and doxycycline (Dox)–inducible knockout (*Intu* KO: $Intu^{f/f}$,$Pax8^{+/-}$,$LC1^{+/-}$) and wild-type (*Intu* WT: $Intu^{f/f}$,$Pax8^{+/-}$,$LC1^{-/-}$ or $Intu^{f/f}$,$Pax8^{-/-}$,$LC1^{+/-}$) mice. **B:** Confirmation of *Intu* knockout efficiency. **Left:** Representative immunoblot of kidney proteins from mice treated with doxycycline and renal IRI for three (3d) and seven (7d) days. **Right:** Immunostaining of acetylated tubulin (Ac-tub) showing shortened cilia in *Intu* KO mice kidneys than in the WT. **C: Left:** Renal histology by hematoxylin and eosin staining. *Intu* KO mice showed more dilated tubules in kidneys than in the WT mice after renal IRI. **Right:** Bar graphs showing the number (**top**) and area (**bottom**) of the dilated tubules in the *Intu* KO and WT mice. **D:** Bar graphs indicating higher blood urea nitrogen (BUN) (**top**) and serum creatinine (SCr) (**bottom**) in *Intu* KO mice than in WT, indicating worse renal recovery after renal IRI in KO mice. $n = 10$ fields of view for WT and KO (**C**); $n = 128$ dilated tubules for WT (**C**); $n = 145$ dilated tubules for KO (**C**); $n = 4$ WT mice (**D**); $n = 3$ KO mice (**D**). $^*P < 0.05$, $^{***}P < 0.001$. Scale bars: 20 μm (**B**); 100 μm (**C**). CTL, control.

xylene/ethanol, followed by incubation with dye solution for 30 minutes at room temperature. Finally, the sections were rinsed with water and mounted for microscopy. Quantification of fibrosis signals was done with ImageJ software version 1.53e (NIH, Bethesda, MD; *http://imagej.nih.gov/ij*, last accessed August 30, 2022).

Immunoblot Analysis

Proteins from kidney tissues and cells were extracted with the SDS lysis buffer, as previously described.[22] Frozen kidney tissues were homogenized in SDS buffer with Bullet Blender Homogenizer (Next Advance, Inc., Troy, NY) for 2 minutes. Extracted samples were centrifuged at 17,000 × *g* for 15 minutes at 4°C to collect supernatant. The samples (50 to 100 μg per lane for tissues; 10 to 15 μg for cultured cells) were electrophoresed in a 10% Bis-Tris gel and transferred to polyvinylidene difluoride membrane (Bio-Rad, Hercules, CA). After blocking with 5% nonfat dry milk (Lab Scientific, Livingston, NJ) in phosphate-buffered saline (PBS) for 1 hour, the membrane was incubated with the primary antibody and washed with PBS/0.1% Tween 20 (MP Biomedicals, Santa Ana, CA). The membrane was finally incubated with the secondary antibody conjugated with horseradish peroxidase for 1 hour at room temperature or overnight at 4°C. The bound antibodies were detected with the Detection Reagent (Pierce, Rockford, IL). Quantification of the band intensity was accomplished with the NIH ImageJ software.

Hematoxylin and Eosin Staining, Immunofluorescence, and Confocal Microscopy

The histology of kidney tissues was examined by hematoxylin and eosin staining. Dilated tubules were counted by the percentage of renal tubules showing a larger tubular lumen than the maximum one in the control. For immunofluorescence staining, tissue antigen retrieval was performed by boiling slides in the retrieval buffer (10 mmol/L sodium citrate, pH 6.0, and 0.05% Tween-20). Cultured cells on coverslips were fixed with 4% paraformaldehyde for 15 minutes, followed by incubation with cold methanol at −20°C. Cells were permeabilized with 0.1% Triton X-100 for 5 minutes if necessary. Samples were incubated with primary

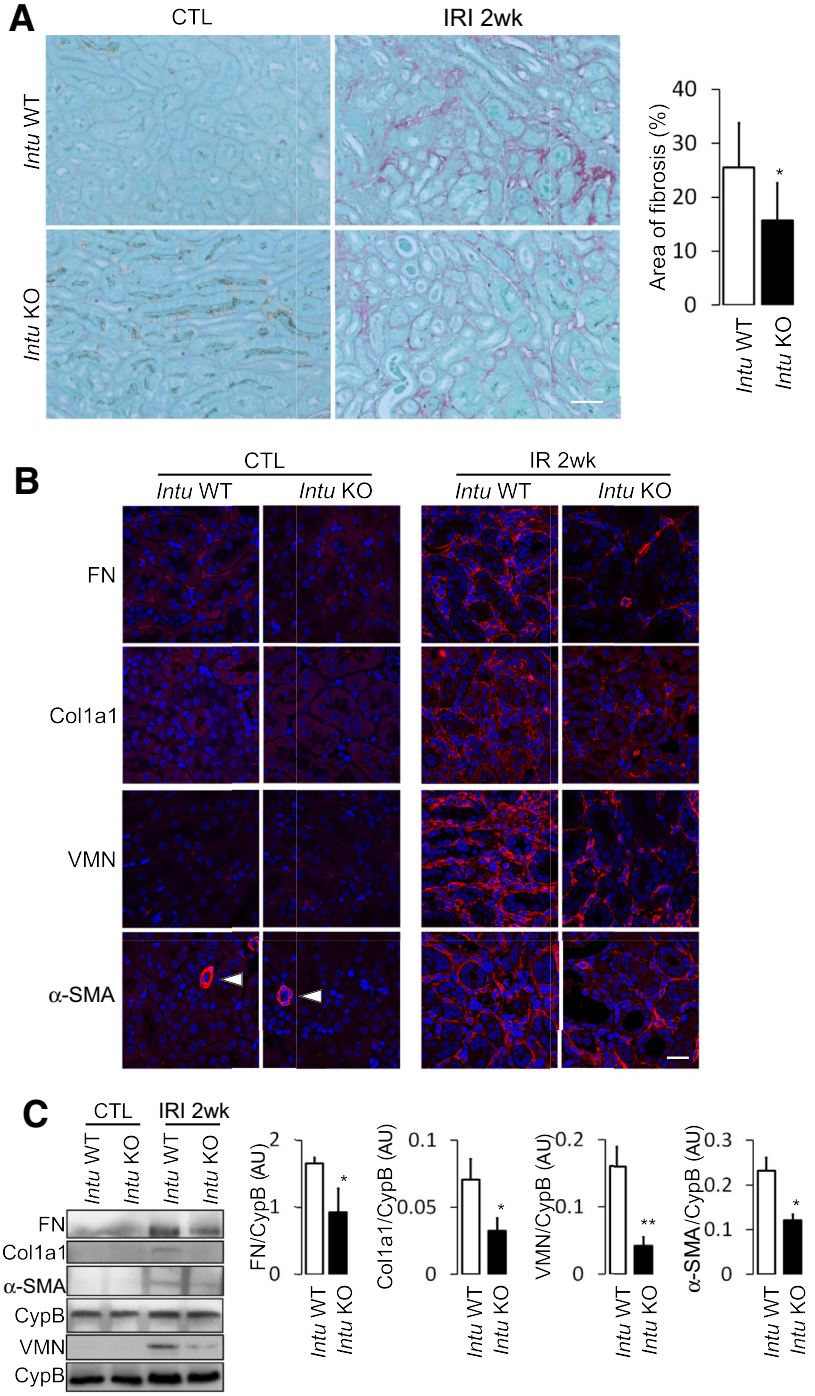

Figure 2 Knockout (KO) of tubular *Intu* suppresses renal fibrosis after ischemia/reperfusion injury (IRI). Renal tubule *Intu* KO mice and wild-type (WT) littermates were subjected to unilateral IRI to collect samples 2 weeks (2wk) later for fibrosis analysis. **A: Left:** Sirius red staining of fibrosis showing less fibrosis in *Intu* KO kidneys than in WT kidneys after renal IRI. **Right:** The staining positive area was evaluated for quantification of fibrosis. **B:** Immunofluorescence of fibronectin (FN), collagen 1a1 (Col1a1), vimentin (VMN), and α-smooth muscle actin 2 (α-SMA), showing less FN and Col1a1 in *Intu* KO kidneys than in WT kidneys after renal IRI. **C:** Immunoblots and densitometry showing less expression of fibrosis marker proteins in *Intu* KO kidneys than in WT kidneys after renal IRI. **Arrowheads**, vasculature structures. $n = 8$ for WT group (**A**); $n = 6$ for KO group (**A**); $n = 3$ mice for *Intu* WT and KO groups (**C**). $^{*}P < 0.05$, $^{**}P < 0.001$. Scale bars: 50 μm (**A**); 10 μm (**B**). AU, arbitrary unit; CTL, control; CypB, cyclophilin B.

antibodies for 1 hour after 1 hour bovine serum albumin blocking, followed by complete washing with PBS, and then incubated with secondary antibodies for another 1 hour. Before mounting with the Prolong Gold antifade reagent without DAPI (P36930; ThermoFisher, Waltham, MA), cell nuclei were stained with Hoechst 33342 (H-1399; Invitrogen, Waltham, MA). Alternatively, samples were mounted with the Prolong Gold antifade reagent with DAPI (P36941; ThermoFisher). For image analysis, Zeiss Axio fluorescence and confocal microscopes (Carl Zeiss Inc., Thornwood, NJ) were used. The confocal microscope was equipped with the LSM Image analysis system.

TUNEL Assay

The *In Situ* Cell Death Detection Kit from Roche (Indianapolis, IN) was used for the terminal deoxynucleotidyl transferase dUTP nick end labeling (TUNEL) assay of

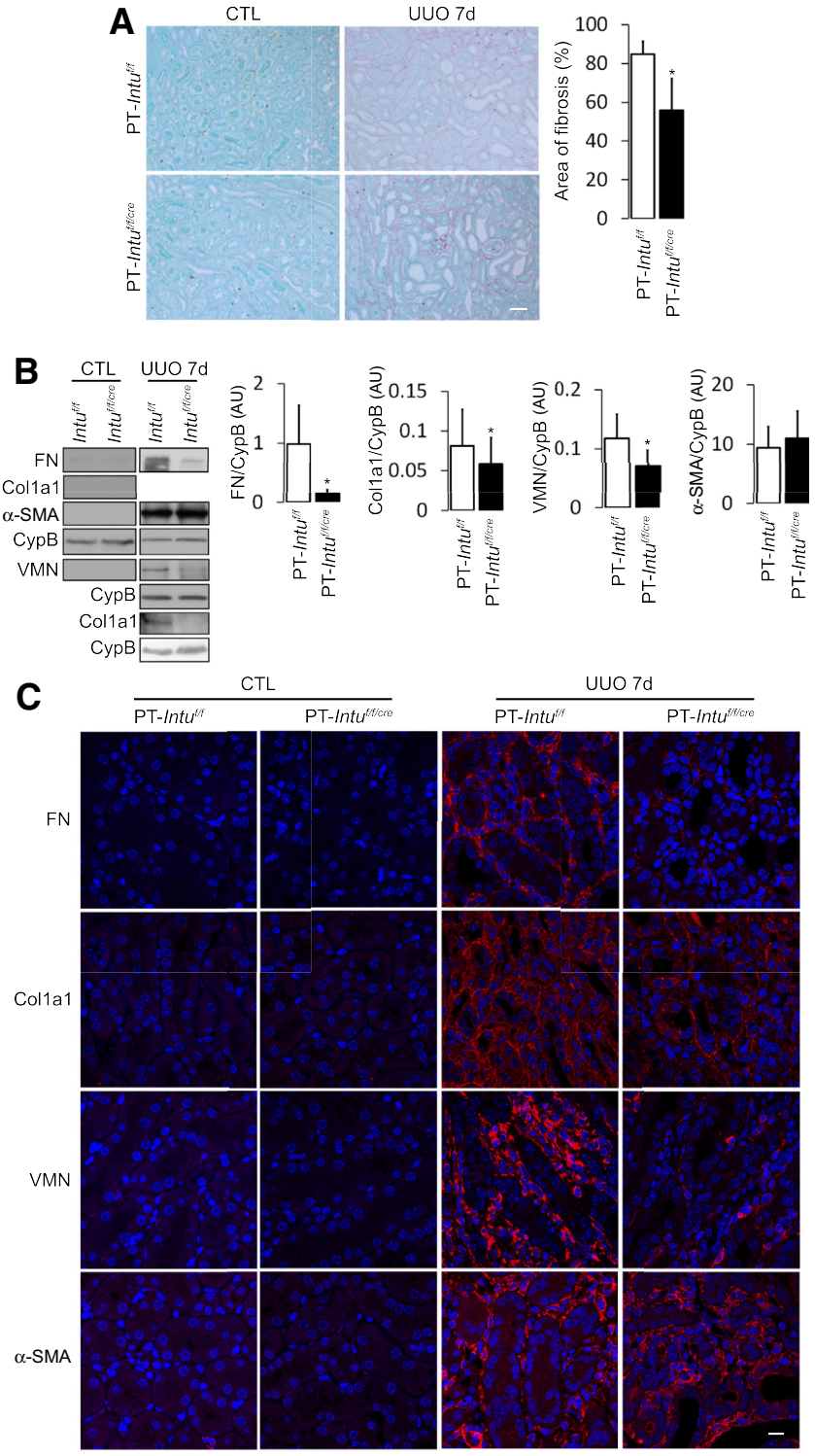

Figure 3 *Intu* knockout (KO) inhibits renal fibrosis induced by unilateral ureteral obstruction (UUO). Proximal tubule–specific *Intu* KO mice (PT-*Intu*$^{f/f/cre}$) and their wild-type (WT) littermates (PT-*Intu*$^{f/f}$) were subjected to UUO for 7 days (UUO 7d) or sham control operation (CTL). **A: Left:** Sirius red staining showing weaker signal in *Intu* KO mice, compared with the WT, after UUO. **Right:** Positive staining area is quantified to show the statistical difference in *Intu* WT and KO mice. **B: Left:** Immunoblots of fibronectin (FN), collagen 1a1 (Col1a1), vimentin (VMN), and α-smooth muscle actin (α-SMA) in kidney tissues. Induction of FN, Col1a1, and VMN, but not α-SMA, during UUO was suppressed in *Intu* KO mice. **Right:** Bar graphs showing the statistical differences of immunoblotting bands quantified by densitometry. **C:** Immunostaining of FN, Col1a1, VMN, and α-SMA, confirming that UUO-associated induction of FN, Col1a1, and VMN, but not α-SMA, was suppressed in *Intu* KO mice. $n = 3$ mice for *Intu* WT and KO groups (**A** and **B**). $^*P < 0.05$. Scale bars: 50 μm (**A**); 10 μm (**C**). AU, arbitrary unit; CypB, cyclophilin B.

kidney tissue sections. Briefly, fixed kidney tissues were embedded in paraffin, divided into sections (7 μm thick; RM2025; Leica, Wetzlar, Germany), and dried overnight before deparaffinization and rehydration through graded concentrations of ethanol. Tissue sections were treated according to the protocol provided by the company.

Immunohistochemistry

Immunohistochemistry was performed as previously described.[26] Kidney sections were treated as described above for antigen retrieval, followed by incubation with blocking buffer (2% bovine serum albumin, 0.2% milk, and

2% normal goat serum in PBS with 0.8% Triton X-100). Tissue sections were incubated with Ki-67 antibody overnight at 4°C, followed by incubation with horseradish peroxidase–conjugated secondary antibody. Signal amplification was performed using the AKOYA TSA Biotin System (Marlborough, MA), and slides were treated with a VECTASTAIN Elite ABC Kit and developed with ImmPACT DAB Peroxidase Substrate (Vector Laboratories, Newark, CA). The reaction was stopped by incubating slides in water. A BZ-X700 fluorescence microscope (KEYENCE, Osaka, Japan) was used for image analysis.

Cell Migration Assay and Quantification of Centrosome Polarization

RPTC cells transfected with *Intu* shRNA or scrambled sequence were cultured in 6-well plates until confluence. Wound was generated by scratching the monolayer cells with a pipette tip. For the migration speed assay, the distance between two edges of the scratch wound at the beginning and at 6 hours was measured, and the migration distance was calculated. For the centrosome reorientation assay, after 10-minute, 4-hour, and 8-hour time points, cells were fixed with 4% paraformaldehyde for 10 minutes and cold methanol at −20°C for 10 minutes. Cells were incubated with γ-tubulin antibody for 1 hour, and after washing with PBS, incubated with secondary antibody conjugated with fluorescence for an additional 1 hour. Cell orientation was determined according to the method described elsewhere.[27] Cells were counted if located in a 120-degree sector facing the wound edge. Sections were mounted with the Prolong Gold antifade reagent with DAPI.

Statistical Analysis

Data are expressed as means ± SD. The *t* test or χ^2 test was used. $P < 0.05$ was considered statistically significant.

Results

Knockout of Tubular *Intu* Suppresses Kidney Repair after IRI

To determine the role of Intu and associated PCP in kidney repair, an inducible *Intu* KO mouse model was established by crossing *Intu*-foxed mice[21] with $Pax8^{+/-}$,$LC1^{+/-}$ mice[23] (Figure 1A). In this model, *Intu* KO can be induced by doxycycline specifically in renal tubules at desired time points. This model was used to knock out *Intu* from renal tubules after acute injury to specifically investigate the effects on kidney repair. Three days of doxycycline treatment did not diminish Intu expression after IRI, but 7 days did

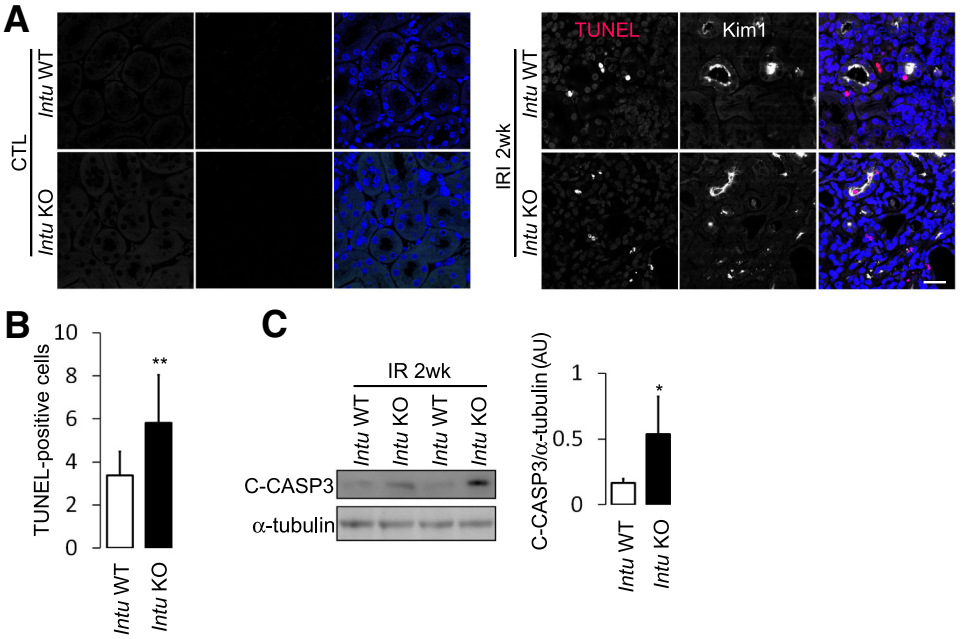

Figure 4 Increased apoptosis in *Intu* knockout (KO) kidneys during maladaptive kidney repair. *Intu* KO mice and wild-type (WT) littermates were subjected to unilateral renal ischemia/reperfusion injury (IRI) for collecting samples 2 weeks (2wk) later for apoptosis analysis. **A** and **B:** Very few terminal deoxynucleotidyl transferase dUTP nick end labeling (TUNEL)–positive cells were found in the sham control (CTL) kidneys of both *Intu* WT and KO mice. At 2 weeks after renal IRI, more TUNEL-positive cells were detected in *Intu* KO kidneys than in WT kidneys. Kim1 was used as a kidney injury marker. For quantification, TUNEL-positive cells were counted in each microscopic field for WT and KO mice. Bar graph shows the statistical difference. **C:** Representative immunoblot and densitometry of cleaved caspase-3 (C-CASP3). $n = 8$ WT mice (**A** and **B**); $n = 6$ KO mice (**A** and **B**); $n = 3$ pairs (**C**). $^*P < 0.05$, $^{**}P < 0.01$. Scale bar = 20 μm (**A**). AU, arbitrary unit.

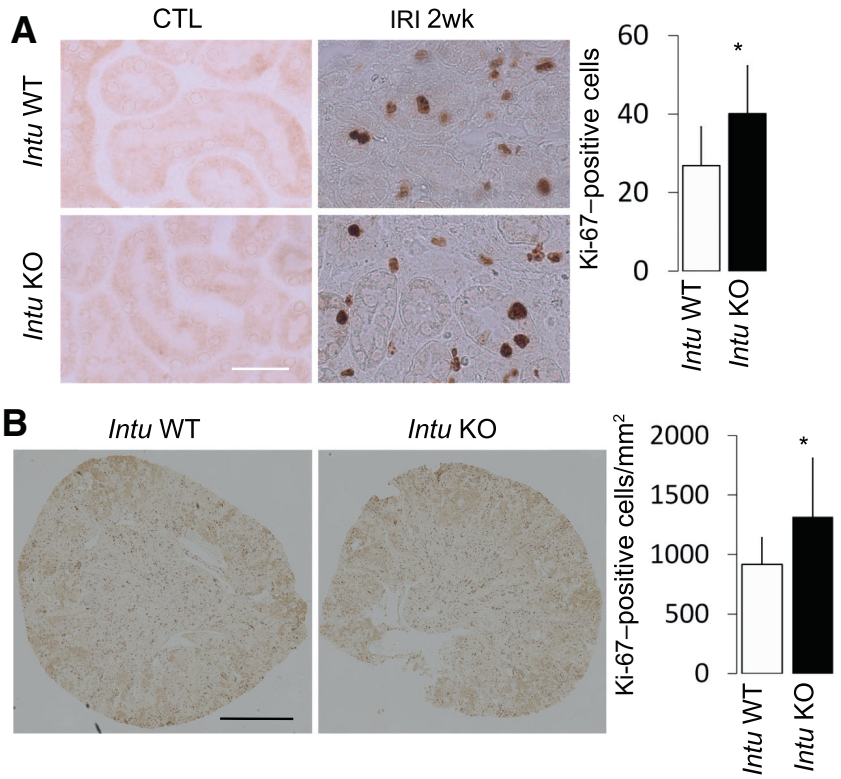

Figure 5 Increased cell proliferation in *Intu* knockout (KO) kidneys during maladaptive kidney repair. *Intu* KO mice and wild-type (WT) littermates were subjected to unilateral renal ischemia/reperfusion injury (IRI) for collecting samples 2 weeks (2wk) later for cell proliferation analysis. **A: Left:** Representative immunostaining for Ki-67 indicating cell proliferation. **Right:** Quantification of Ki-67–positive cells from randomly chosen fields of view for the WT and KO mice. A statistical difference was found between these two groups after IRI. **B: Left:** KEYENCE microscopy scan of sections to count all the Ki-67–positive cells. **Right:** Quantification of Ki-67–positive cells indicating more apoptotic cells in *Intu* KO mice than in WT mice. $n = 8$ WT mice (**A**); $n = 6$ KO mice (**A**). $^*P < 0.05$. Scale bars: 50 μm (**A**); 500 μm (**B**). CTL, control.

(Figure 1B). The KO effect was further confirmed by examining primary cilia. Cilium length and frequency were all significantly diminished in *Intu* KO mouse kidneys (Figure 1B). To examine the effect of *Intu* KO on kidney repair, renal histology was analyzed by hematoxylin and eosin staining after renal IRI (Figure 1C). Two weeks after renal IRI, *Intu* KO mouse kidneys had more dilated tubules and larger areas of dilation than wild-type kidneys. Functionally, both blood urea nitrogen and serum creatinine were higher in KO mice than in wild-type mice (Figure 1D). These results indicate that KO of *Intu* from renal tubules suppresses kidney repair after renal IRI.

Knockout of Tubular *Intu* Suppresses Renal Fibrosis after IRI

Sirius red and fast green staining was used to evaluate fibrosis in wild-type and KO mice. Sirius red signal in *Intu* KO kidneys was weaker than in the wild-type kidneys after 2 weeks of ischemia/reperfusion (Figure 2A), whereas Sirius red signal in control kidneys (wild type and KO) was negligible. Additional approaches such as immunostaining and immunoblotting were used to examine components of extracellular matrix composition. With antibodies to fibronectin and collagen 1a1, decreased fibronectin and collagen staining was found in *Intu* KO mice versus the wild-type mice after 2 weeks of ischemia/reperfusion (Figure 2B). In *Intu* KO kidneys, the staining of two myofibroblast markers (vimentin and α-smooth muscle actin) was reduced in comparison to that in the wild-type kidneys. These findings were further confirmed by immunoblotting (Figure 2C).

Intu Knockout Inhibits Renal Fibrosis Induced by UUO

To determine whether fibrosis inhibition in *Intu* KO kidneys was also observed in other fibrosis models, renal fibrosis was introduced by UUO in a proximal tubule–specific *Intu* KO mouse model. UUO is a common model to study kidney fibrosis; it rapidly causes reduced renal blood flow and glomerular filtration rate, interstitial inflammation, tubule dilation, and fibrosis.[28] Sirius red signal was significantly reduced in *Intu* KO mice versus the wild type after 7-day UUO (Figure 3A). After 7-day UUO, fibronectin and collagen expression levels were increased in *Intu* wild-type and KO mice, particularly in the former, whereas in control mice, fibronectin and collagen were hardly detected (Figure 3B). Vimentin expression was reduced in *Intu* KO versus the wild type, whereas α-smooth muscle actin was slightly increased, although no statistical significance was found. Immunostaining with antibodies to fibronectin, collagen 1a1, vimentin, and α-smooth muscle actin indicated results similar to those obtained by immunoblotting (Figure 3C).

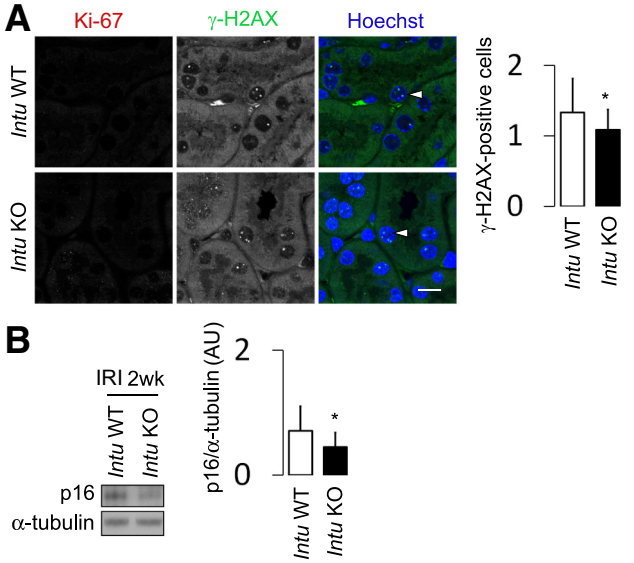

Figure 6 Suppressed senescence in *Intu* knockout (KO) kidneys during maladaptive kidney repair. *Intu* KO mice and wild-type (WT) littermates were subjected to unilateral renal ischemia/reperfusion injury (IRI). Cell senescence analysis was performed two weeks (2wk) later. **A: Left:** γ-H2AX staining of senescent cells (**arrowheads**). **Right:** The cells with more than four γ-H2AX foci were counted in randomly selected fields to quantify senescence in *Intu* WT and KO kidney tissue sections. **B:** Immunoblot (**left**) and densitometry (**right**) of p16. $n = 27$ WT kidney tissue sections (**A**); $n = 23$ KO kidney tissue sections (**A**). $^*P < 0.05$. Scale bar = 10 μm (**A**). AU, arbitrary unit.

Higher Levels of Apoptosis in *Intu* Knockout Kidneys during Maladaptive Kidney Repair

To determine apoptosis in *Intu* mice, TUNEL assay was performed on kidney sections. In comparison to the control kidneys with no signal, more TUNEL-positive cells were found in *Intu* KO kidneys than in the wild type (Figure 4, A and B). Kim1, a marker for kidney injury, was found in both wild-type and KO kidneys. After 2 weeks of ischemia/reperfusion, more cleaved caspase-3 was found in *Intu* KO kidneys than in the wild-type kidneys, which was consistent with TUNEL staining (Figure 4C).

Higher Levels of Cell Proliferation in *Intu* Knockout Kidneys during Maladaptive Kidney Repair

To define cell proliferation in *Intu* mice, immunohistochemistry with antibody against Ki-67, a cell proliferation marker, was performed on kidney sections. A random count of Ki-67−positive cells indicated a higher number in *Intu* KO kidneys than in the wild-type kidneys (Figure 5A). To more accurately count positive cells, a KEYENCE microscope was used to scan the whole sections with appropriate software. The results further confirmed the presence of more proliferating cells in *Intu* KO kidneys than in the wild-type kidneys (Figure 5B).

Suppressed Senescence in *Intu* Knockout Kidneys during Maladaptive Kidney Repair

Because increased proliferation and apoptosis are usually accompanied by more severe fibrosis, whether there was an alternative mechanism for the suppression of fibrosis in *Intu* KO mice was studied. To study senescence in *Intu* wild-type and KO kidney cells, immunostaining with antibodies against Ki-67 and γ-H2AX was performed. A large majority of tubular cells containing one to three foci in the nuclei with positive staining for Ki-67 were found. A small proportion of cells with more than four foci in the nucleus and negative Ki-67 staining were counted as senescent cells. There were fewer senescent cells in *Intu* KO kidneys than in the *Intu* wild-type kidneys (Figure 6A), suggesting a suppression of senescence in *Intu* KO kidneys. This finding was further confirmed by immunoblotting with p16 antibody (Figure 6B). The p16 expression was lower in *Intu* KO than in the wild type.

Intu Knockdown Retards Scratch Wound Healing in Cultured Proximal Tubular Cells

To define the role of Intu in would healing, stable *Intu* knockdown cells were generated by transfecting *Intu* siRNA in RPTC cells, a rat proximal tubular epithelial cell line (Figure 7A). Knockdown cells demonstrated slower migration on the scratch assay (Figure 7, B and C). Centrosome orientation was examined next at 10-minute, 4-hour, and 8-hour intervals after cell wound. After 10 minutes, only a small percentage of cells oriented toward the wound, and no difference was found between control and *Intu* knockdown cells (Figure 7D). After 4 or 8 hours, fewer *Intu* knockdown cells reoriented toward the wound, suggesting the dysfunction of centrosome orientation in *Intu* knockdown cells. Primary cilium length was shorter in *Intu* knockdown cells than in the control cells (Figure 7E).

Discussion

Kidney repair after injury involves the differentiation, migration, proliferation, and redifferentiation of surviving tubular cells to reconstruct functional renal tubules. We hypothesized that cell division during kidney repair should be oriented longitudinally along the tubule via PCP, because otherwise cell proliferation may lead to the expansion of tubular lumen, resulting in cyst formation. To test this possibility, in this study, the role of PCP was determined in kidney repair by ablating the key PCP effector gene *Intu* from renal tubular cells. A doxycycline-inducible mouse model was generated to delete *Intu* from renal tubules after ischemic kidney injury, which was used to specifically study the involvement of Intu-associated PCP in tubular repair, renal recovery, and fibrosis. Knockout of *Intu* from renal tubular cells delayed renal recovery and suppressed

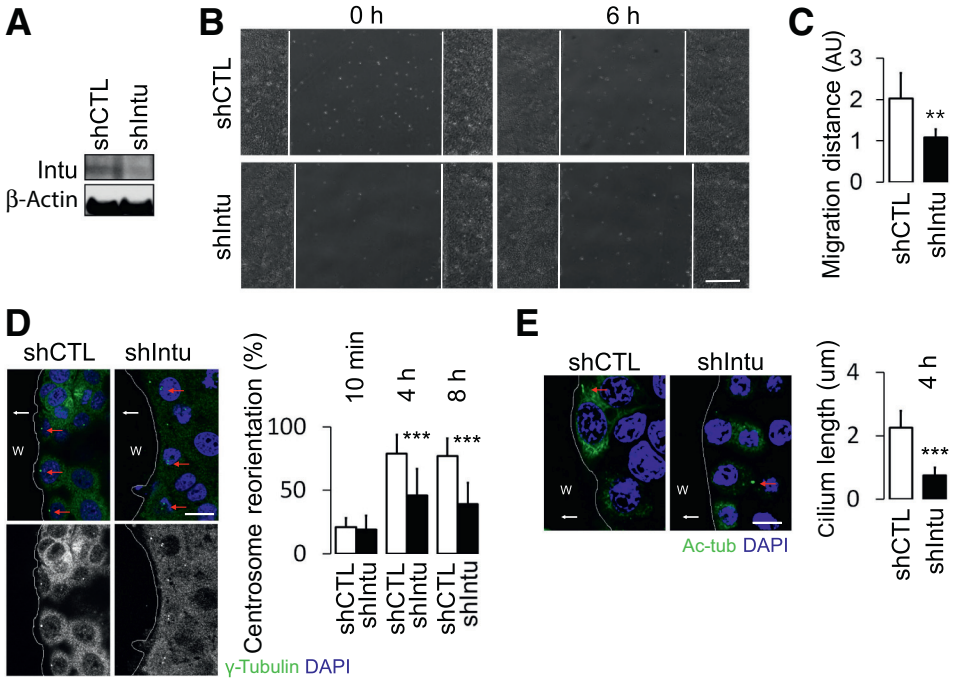

Figure 7 *Intu* knockdown retards scratch wound (W) healing in cultured proximal tubular cells. RPTC cells were stably transfected with *Intu* shRNA (shIntu) or control sequence (shCTL). A scratch wound was generated in the monolayer of cultured cells to observe closure of the wound at indicated time points. **A:** *Intu* knockdown by shIntu was confirmed by immunoblotting. **B:** Representative images showing slower wound closure in *Intu* knockdown cells than in control transfection cells at 6 hours. **C:** Bar graph showing the wound edge migration distance. **D: Left:** γ-Tubulin immunostaining to show centrosome reorientation during wound healing. **Right:** The cells with centrosomes facing the wound were counted and quantified by percentage to total cells. After 4 and 8 hours of wound healing, fewer cells with centrosome facing to the wound were noticed in *Intu* knockdown cells in comparison to the control transfection cells. Green channel is shown in grayscale. The approximate edge of the wound is shown by a **white line**. **E: Left:** Acetylated tubulin (Ac-tub) immunostaining to show cilium length. **Right:** Cilium length was shorter in Intu knockdown cells than in the controls after 4 hours of wound healing. **D** and **E: Red arrows** indicate either centrioles (**D**) or primary cilia (**E**). **White arrows**, migration direction. $n = 11$ Intu knockdown cells (**E**); $n = 10$ controls (**E**). $^{**}P < 0.01$, $^{***}P < 0.001$. Scale bars: 250 μm (**B**); 10 μm (**D** and **E**). AU, arbitrary unit.

fibrogenesis during maladaptive kidney repair, supporting a role of PCP in tubular repair after kidney injury.

PCP proteins were originally recognized for their roles in regulating tissue polarity. Recently, some PCP proteins have been localized to primary cilia and basal body/centriole,[18,19,29,30] whereas defective PCP was reported in polycystic kidney disease.[17] The effector protein Intu is located in the primary cilia and basal body/centriole areas. Recent work showed that depletion of Intu sensitizes kidney to ischemia/reperfusion injury.[22] The present study demonstrated that Intu plays an essential role in tubular repair and renal recovery after kidney injury. These results support the potential of kidney protection and improvement of kidney repair by maintaining Intu and promoting ciliogenesis and PCP.

Renal interstitial fibrosis is a pathologic characteristic of progressive kidney disease that is often accompanied by worsened renal function.[31,32] In the current study, knockout of tubular *Intu* delayed renal recovery and repair, but it suppressed the development of renal fibrosis after ischemia/reperfusion injury. This observation was somewhat surprising, because worse fibrosis was expected in *Intu* KO mice as they had poorer kidney repair than in wild-type mice. The inhibitory effect of *Intu* KO on renal fibrosis was further verified using the UUO model. This observation indicates that, although renal interstitial fibrosis is a pathologic feature of maladaptive kidney repair, it may not play a causative role in the delayed tubular repair and renal recovery. Such a notion is consistent with the fact that the function of a kidney mainly depends on the number and efficacy of the nephron, which consist of a glomerulus with associated renal tubules. In this regard, excessive fibrosis may adversely affect the nephron function, but mild to moderate levels of fibrosis may not. Selective ablation of fibroblasts in mice has been shown to trigger kidney injury and attenuated tubular regeneration during UUO, implying a beneficial effect of fibroblasts in kidney repair.[33] In line with these observations, the focus on fibrosis in chronic or progressive kidney disease has recently been questioned.[34]

To understand the effects of *Intu* knockout on kidney repair and fibrosis, cell proliferation, apoptosis, and senescence were analyzed in kidney tissues. Knockout of *Intu* from renal tubules increased apoptosis as well as proliferation after renal IRI. The observed higher level of apoptosis in *Intu* KO kidneys is consistent with their delayed recovery. However, a higher level of proliferation may suggest

active kidney repair. The higher level of proliferation was likely caused by existing tubular damage, as shown by apoptosis in *Intu* KO mice. This indicates that wild-type kidneys may have better repair at 2 weeks after renal IRI and, thus, less apoptosis and less tubular cell proliferation. Proliferative and apoptotic cells were found not only in tubular cells but also spread to nontubular areas. This finding suggests that *Intu* knockout in tubular cells has roles in cell proliferation and apoptosis beyond the tubular epithelial cells. The cross talk between tubular epithelial cells and interstitial cells is critical to maladaptive kidney repair.[6,7,35,36] Especially, injured tubular cells produce a multitude of cytokines for the recruitment and simulation of inflammatory cells and fibroblasts. In the present study, knockout of *Intu* in tubular cells may affect the production and secretion of these cytokines for extratubular apoptosis and proliferation.

Many factors (eg, inflammation, oxidative stress, autophagy, apoptosis, metabolism, and senescence) contribute to renal fibrosis.[37–39] Among these, senescence is emerging as an important factor. Senescence suppresses renal regeneration and senescence inhibitors improve renal recovery and kidney repair after AKI.[40] In the present study, *Intu* knockout kidneys had fewer senescent cells and lower expression of senescence markers, like p16, during maladaptive kidney repair after renal IRI (Figure 6). Therefore, it is possible that knockout of tubular *Intu* suppresses renal fibrosis by preventing the development of the senescence phenotype in tubular cells.

Mechanistically, how PCP modulates the repair or reconstruction of tubules after kidney injury is still unknown. However, PCP proteins have been known to play a significant role in cell migration and wound healing.[13] For instance, wdpcp, a PCP protein, regulates cell migration and cell polarity through cytoskeleton.[30] Similarly, primary cilia also play a crucial role in cell migration.[41] Because proximal tubules are repaired mainly by the survival epithelial cells after kidney injury, the present study examined the effect of *Intu* knockdown on wound healing in renal proximal tubular cells.[42] *Intu* knockdown cells had a lower percentage of centrosome reorientation facing the wound, which was associated with slower migration. In addition, *Intu* knockdown cells bear shortened primary cilia. Thus, both disorientation of centrosome and shortened primary cilia in *Intu* knockdown cells may contribute to the slower migration and wound healing, which to some extent mimics renal tubule repair after kidney injury.

In summary, data from the present study corroborated the observation that Intu, a key effector protein of PCP, plays a protective role in AKI model, and showed that it also affects renal recovery and tubular repair after kidney injury. In addition, knockout of *Intu* in kidney tubules suppressed renal fibrosis through a likely senescence-associated mechanism, accompanied by increased cell proliferation and apoptosis. In cultured renal tubular cells, *Intu* knockdown slowed down cell migration and bore a lower percentage of centrosomes toward the wound, suggesting a function of PCP in tubular repair.

Acknowledgments

We thank Dr. Robert Koesters (Heidelberg University) for providing the inducible *Cre* mouse strain; and Dr. Volker Haase (Vanderbilt University School of Medicine) for providing the *PEPCK-Cre* mouse strain.

References

1. Agarwal A, Dong Z, Harris R, Murray P, Parikh SM, Rosner MH, Kellum JA, Ronco C: Cellular and molecular mechanisms of AKI. J Am Soc Nephrol 2016, 27:1288–1299
2. Basile DP, Bonventre JV, Mehta R, Nangaku M, Unwin R, Rosner MH, Kellum JA, Ronco C, Group AXW: Progression after AKI: understanding maladaptive repair processes to predict and identify therapeutic treatments. J Am Soc Nephrol 2016, 27:687–697
3. Hsu CY: Yes, AKI truly leads to CKD. J Am Soc Nephrol 2012, 23: 967–969
4. Linkermann A, Chen G, Dong G, Kunzendorf U, Krautwald S, Dong Z: Regulated cell death in AKI. J Am Soc Nephrol 2014, 25: 2689–2701
5. Bonventre JV, Yang L: Cellular pathophysiology of ischemic acute kidney injury. J Clin Invest 2011, 121:4210–4221
6. Ferenbach DA, Bonventre JV: Mechanisms of maladaptive repair after AKI leading to accelerated kidney ageing and CKD. Nat Rev Nephrol 2015, 11:264–276
7. Venkatachalam MA, Weinberg JM, Kriz W, Bidani AK: Failed tubule recovery, AKI-CKD transition, and kidney disease progression. J Am Soc Nephrol 2015, 26:1765–1776
8. Fu Y, Xiang Y, Li H, Chen A, Dong Z: Inflammation in kidney repair: mechanism and therapeutic potential. Pharmacol Ther 2022, 237:108240
9. Simons M, Mlodzik M: Planar cell polarity signaling: from fly development to human disease. Annu Rev Genet 2008, 42:517–540
10. Adler PN: Planar signaling and morphogenesis in Drosophila. Dev Cell 2002, 2:525–535
11. Peng Y, Axelrod JD: Asymmetric protein localization in planar cell polarity: mechanisms, puzzles, and challenges. Curr Top Dev Biol 2012, 101:33–53
12. Wallingford JB: Planar cell polarity and the developmental control of cell behavior in vertebrate embryos. Annu Rev Cell Dev Biol 2012, 28:627–653
13. Carroll TJ, Yu J: The kidney and planar cell polarity. Curr Top Dev Biol 2012, 101:185–212
14. McNeill H: Planar cell polarity and the kidney. J Am Soc Nephrol 2009, 20:2104–2111
15. Seifert JR, Mlodzik M: Frizzled/PCP signalling: a conserved mechanism regulating cell polarity and directed motility. Nat Rev Genet 2007, 8:126–138
16. Torban E, Sokol SY: Planar cell polarity pathway in kidney development, function and disease. Nat Rev Nephrol 2021, 17:369–385
17. Fischer E, Legue E, Doyen A, Nato F, Nicolas JF, Torres V, Yaniv M, Pontoglio M: Defective planar cell polarity in polycystic kidney disease. Nat Genet 2006, 38:21–23
18. Toriyama M, Lee C, Taylor SP, Duran I, Cohn DH, Bruel AL, Tabler JM, Drew K, Kelly MR, Kim S, Park TJ, Braun D, Pierquin G, Biver A, Wagner K, Malfroot A, Panigrahi I, Franco B, Al-Lami HA, Yeung Y, Choi YJ, Duffourd Y, Faivre L, Riviere JB, Chen J, Liu KJ, Marcotte EM, Hildebrandt F, Thauvin-Robinet C, Krakow D, Jackson PK, Wallingford JB: The ciliopathy-associated CPLANE

proteins direct basal body recruitment of intraflagellar transport machinery. Nat Genet 2016, 48:648−656
19. Yasunaga T, Hoff S, Schell C, Helmstadter M, Kretz O, Kuechlin S, Yakulov TA, Engel C, Muller B, Bensch R, Ronneberger O, Huber TB, Lienkamp SS, Walz G: The polarity protein Inturned links NPHP4 to Daam1 to control the subapical actin network in multiciliated cells. J Cell Biol 2015, 211:963−973
20. Park TJ, Haigo SL, Wallingford JB: Ciliogenesis defects in embryos lacking inturned or fuzzy function are associated with failure of planar cell polarity and Hedgehog signaling. Nat Genet 2006, 38: 303−311
21. Zeng H, Hoover AN, Liu A: PCP effector gene Inturned is an important regulator of cilia formation and embryonic development in mammals. Dev Biol 2010, 339:418−428
22. Wang S, Liu A, Wu G, Ding HF, Huang S, Nahman S, Dong Z: The CPLANE protein Intu protects kidneys from ischemia-reperfusion injury by targeting STAT1 for degradation. Nat Commun 2018, 9:1234
23. Traykova-Brauch M, Schonig K, Greiner O, Miloud T, Jauch A, Bode M, Felsher DW, Glick AB, Kwiatkowski DJ, Bujard H, Horst J, von Knebel Doeberitz M, Niggli FK, Kriz W, Grone HJ, Koesters R: An efficient and versatile system for acute and chronic modulation of renal tubular function in transgenic mice. Nat Med 2008, 14:979−984
24. Livingston MJ, Shu S, Fan Y, Li Z, Jiao Q, Yin XM, Venkatachalam MA, Dong Z: Tubular cells produce FGF2 via autophagy after acute kidney injury leading to fibroblast activation and renal fibrosis. Autophagy 2022, 19:256−277
25. Rankin EB, Tomaszewski JE, Haase VH: Renal cyst development in mice with conditional inactivation of the von Hippel-Lindau tumor suppressor. Cancer Res 2006, 66:2576−2583
26. Wang S, Zhuang S, Dong Z: IFT88 deficiency in proximal tubular cells exaggerates cisplatin-induced injury by suppressing autophagy. Am J Physiol Renal Physiol 2021, 321:F269−F277
27. Bisel B, Wang Y, Wei JH, Xiang Y, Tang D, Miron-Mendoza M, Yoshimura S, Nakamura N, Seemann J: ERK regulates Golgi and centrosome orientation towards the leading edge through GRASP65. J Cell Biol 2008, 182:837−843
28. Yang HC, Zuo Y, Fogo AB: Models of chronic kidney disease. Drug Discov Today Dis Models 2010, 7:13−19
29. Zilber Y, Babayeva S, Seo JH, Liu JJ, Mootin S, Torban E: The PCP effector Fuzzy controls cilial assembly and signaling by recruiting Rab8 and Dishevelled to the primary cilium. Mol Biol Cell 2013, 24: 555−565
30. Cui C, Chatterjee B, Lozito TP, Zhang Z, Francis RJ, Yagi H, Swanhart LM, Sanker S, Francis D, Yu Q, San Agustin JT, Puligilla C, Chatterjee T, Tansey T, Liu X, Kelley MW, Spiliotis ET, Kwiatkowski AV, Tuan R, Pazour GJ, Hukriede NA, Lo CW: Wdpcp, a PCP protein required for ciliogenesis, regulates directional cell migration and cell polarity by direct modulation of the actin cytoskeleton. PLoS Biol 2013, 11:e1001720
31. Humphreys BD: Mechanisms of renal fibrosis. Annu Rev Physiol 2018, 80:309−326
32. Li L, Fu H, Liu Y: The fibrogenic niche in kidney fibrosis: components and mechanisms. Nat Rev Nephrol 2022, 18:545−557
33. Nakamura J, Sato Y, Kitai Y, Wajima S, Yamamoto S, Oguchi A, Yamada R, Kaneko K, Kondo M, Uchino E, Tsuchida J, Hirano K, Sharma K, Kohno K, Yanagita M: Myofibroblasts acquire retinoic acid-producing ability during fibroblast-to-myofibroblast transition following kidney injury. Kidney Int 2019, 95:526−539
34. Safirstein R: A clear pathway to tubulointerstitial disease: is an exclusive focus on fibrosis justified? J Clin Invest 2021, 131:e144803
35. Wang Y, Chang J, Yao B, Niu A, Kelly E, Breeggemann MC, Abboud Werner SL, Harris RC, Zhang MZ: Proximal tubule-derived colony stimulating factor-1 mediates polarization of renal macrophages and dendritic cells, and recovery in acute kidney injury. Kidney Int 2015, 88:1274−1282
36. Huen SC, Huynh L, Marlier A, Lee Y, Moeckel GW, Cantley LG: GM-CSF promotes macrophage alternative activation after renal ischemia/reperfusion injury. J Am Soc Nephrol 2015, 26:1334−1345
37. Docherty MH, O'Sullivan ED, Bonventre JV, Ferenbach DA: Cellular senescence in the kidney. J Am Soc Nephrol 2019, 30: 726−736
38. Lv W, Booz GW, Fan F, Wang Y, Roman RJ: Oxidative stress and renal fibrosis: recent insights for the development of novel therapeutic strategies. Front Physiol 2018, 9:105
39. Zhao XC, Livingston MJ, Liang XL, Dong Z: Cell apoptosis and autophagy in renal fibrosis. Adv Exp Med Biol 2019, 1165: 557−584
40. Mylonas KJ, O'Sullivan ED, Humphries D, Baird DP, Docherty MH, Neely SA, Krimpenfort PJ, Melk A, Schmitt R, Ferreira-Gonzalez S, Forbes SJ, Hughes J, Ferenbach DA: Cellular senescence inhibits renal regeneration after injury in mice, with senolytic treatment promoting repair. Sci Transl Med 2021, 13:eabb0203
41. Veland IR, Lindbaek L, Christensen ST: Linking the primary cilium to cell migration in tissue repair and brain development. Bioscience 2014, 64:1115−1125
42. Humphreys BD, Valerius MT, Kobayashi A, Mugford JW, Soeung S, Duffield JS, McMahon AP, Bonventre JV: Intrinsic epithelial cells repair the kidney after injury. Cell Stem Cell 2008, 2:284−291